Seismic analysis of the Roman Temple of Évora, Portugal

D.V. Oliveira
ISISE, University of Minho, Guimarães, Portugal

G. Grecchi, A. McCall, J. Noh, E. Speer & M. Tohidi
University of Minho, Guimarães, Portugal

SUMMARY
The Roman temple of Évora dates back to the 1st century AD and has undergone several changes throughout history, including various additions, which have been removed. Several archaeological studies have recently been carried out, but the structural safety of the temple is unknown. Of particular concern is the temple's seismic resistance, as it is located in a region subjected to a moderate seismic hazard.

The main purpose of this paper is to ascertain the temple's behaviour under seismic excitation through limit analysis and discrete element analysis. Both analysis techniques will use the assumption that the structure is composed of rigid blocks connected with dry joints. Geometric information has been derived from a recent laser scanning surveying, while calibration undertaken using in-situ results from GPR and dynamic identification tests. The main results are presented and discussed in detail as well as the need for possible repair works within the framework of the ICARSAH guidelines.

Keywords: Roman temple, seismic safety, limit analysis, DEM analysis.

1. INTRODUCTION

The Roman temple analysed here is located in the historic city centre of Évora, Portugal. Évora, which is the capital of the Alentejo province in the south of Portugal, is thought to date back to Celtic times. In 57 BC, the city was conquered by the Romans who renamed the city Liberalitas Julia and signs of their presence can still be seen around the town today. The construction of the temple began in the 1st century AD during the time of Emperor Augustus in the Forum of Évora and was finished between the 2nd and 3rd centuries. It is understood that the temple was partly destroyed by the Visigoths during the 5th century. During the 14th century, walls were constructed between the outer columns and the temple was then linked to Évora castle and used as defensive tower until the 18th century, as detailed in the various works of German archaeologist Theodor Hauschild (1982-1997). One of the most recent uses of the temple was as a butcher's shop. As late as the 19th century, pyramid shaped merlons could still be seen at the heads of the outer walls, as illustrated in Figure 1(a).

Between 1870 and 1871, considerable intervention was carried out on the temple by Giuseppe Cinatti, a follower of Violet Le-Duc's theories on intervention, as discussed by Rodrigues (2000). However, in the case of the Évora temple, it seems he had followed Ruskin's intervention theory of allowing the structure to naturally deteriorate. It is thought that the main reason that pushed Cinatti not to reconstruct the temple was because the temple had deteriorated to such an extent that it was not possible to accurately restore the temple to its condition from pagan times. Therefore, it was decided to re-create the ruin and give residents and visitors an insight into the Roman history of Évora. Rather than reconstructing the pagan temple, the walls (which had been added between the columns) were removed. Although the walls between columns were not original, it is quite certain that they helped to ensure the survival of the temple, most notably through the Lisbon earthquake of 1755. At the time of the intervention, an inventory was also made of missing sections of the temple, the podium was

surveyed and inspected, and some beam sections were connected with iron ties for safety. A section of frieze found in the city hall was also returned to the temple and the entire temple underwent a cleaning regime. Furthermore, the plaza around the podium was paved, and a metallic barrier was fixed at one end of the temple to prevent people from entering the podium.

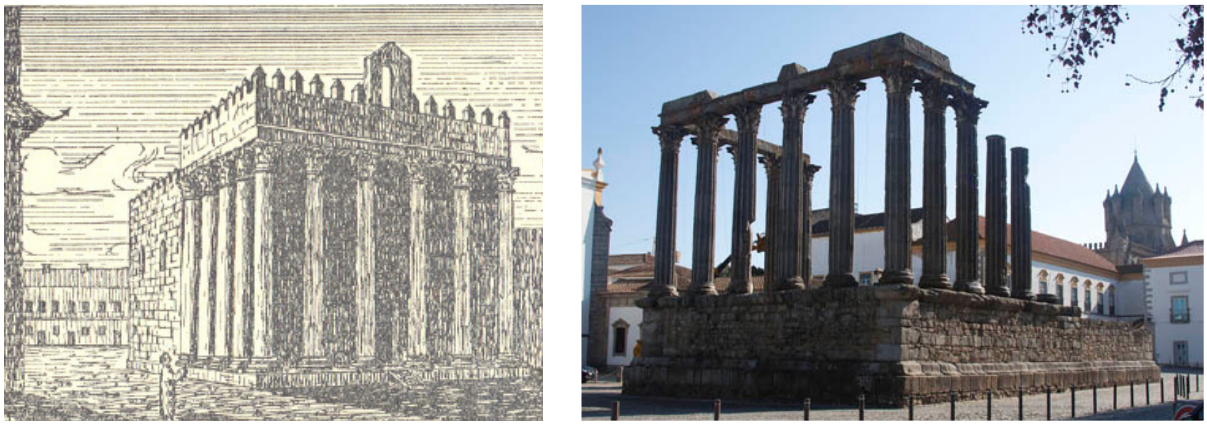

(a) (b)

Figure 1. The Roman temple of Évora: (a) in 1795 before Cinatti's restoration (Pereira 1934); (b) in its current state.

The remains of the temple in Évora consist of 14 hexastyle columns (originally 32 columns in a peripteros layout) which are approximately 90 cm in diameter, see also Figure 1(b). The columns sit on a podium 3.5 m high, 15 m wide and 25 m long. Since the column drum heights vary and are not consistent throughout the structure, it is understood that the columns were originally covered in stucco to hide the imperfections. However, this stucco was misunderstood as an intervention measure and was removed.

The stone used to construct the temple has previously been analysed by Lopes et al. (2000) using a petrographic technique. The analysis concluded that the columns and architrave are made of local granite and the capitals and column bases of marble from nearby Estremoz. Studies by Hauschild (1982, 1986, and 1997) have also revealed the presence of water channels on three sides of the building. A great deal of conjecture still remains around the layout of the temple and the position of the staircase. One idea is that the staircase was positioned centrally at the front of the building running perpendicular to the façade. Alternatively, the staircase may have run parallel to the front of the building or there may have been a combination of both layouts. Archaeologists are still debating this topic, as there is not conclusive evidence for any of the layouts.

2. IN-SITU TESTS

2.1. Visual inspection

A visual inspection was carried out in order to check the damage level of the temple and to confirm its geometry. It was found that the most damaged columns are the two front central columns where a door was previously fixed when the temple was used as the tower of Évora Castle. Generally, the other remaining columns are in good condition, however some of the marble bases have separated into two pieces. Some of the capitals have missing parts of their decorations, but it is not thought to compromise their stability. Also the degree of biological colonization was checked. Mainly, this is a result of the growth of lichen, algae, and moss, which is easily visible throughout the temple. The most severely affected areas are the bases of the columns, which exhibit a range of moss and fungus growth. However, due to the lighter colour of marble compared to the granite, biological growth on the capitals and bases is more obvious. Examples of damage and biological colonization maps can be seen in Figure 2**.**

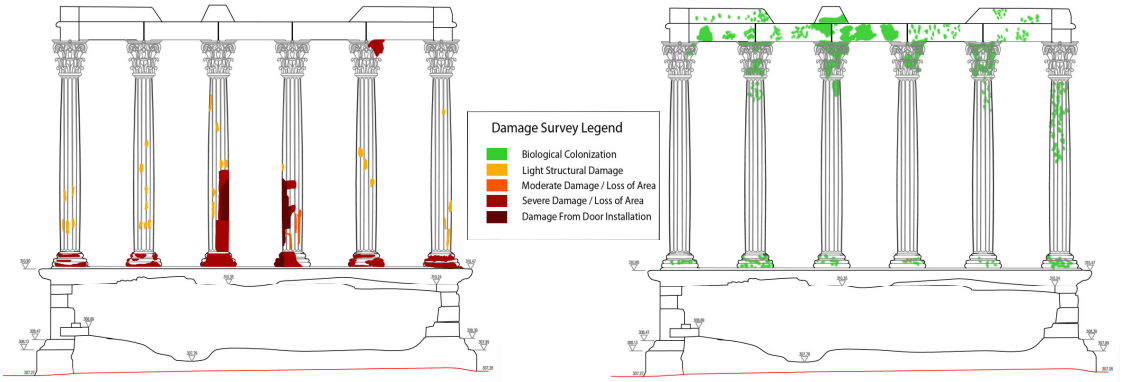

(a) (b)

Figure 2. Damage survey: (a) structural damage and loss of area (b) biological colonization.

2.2. Ground penetration test

Ground penetrating radar (GPR) tests have also been performed and as a result it's thought that there are no connections between column drums, but steel connectors were detected between several architraves, see also Figure 3. It was not possible to survey all architrave joints, but it seemed that most of the architraves have been connected using steel elements. Holes in the sides of the stones used on the top outer edge of the podium were also noticed, and a small focused investigation lead to the conclusion that these stone pieces around the temple were most likely interlocked through some connected elements.

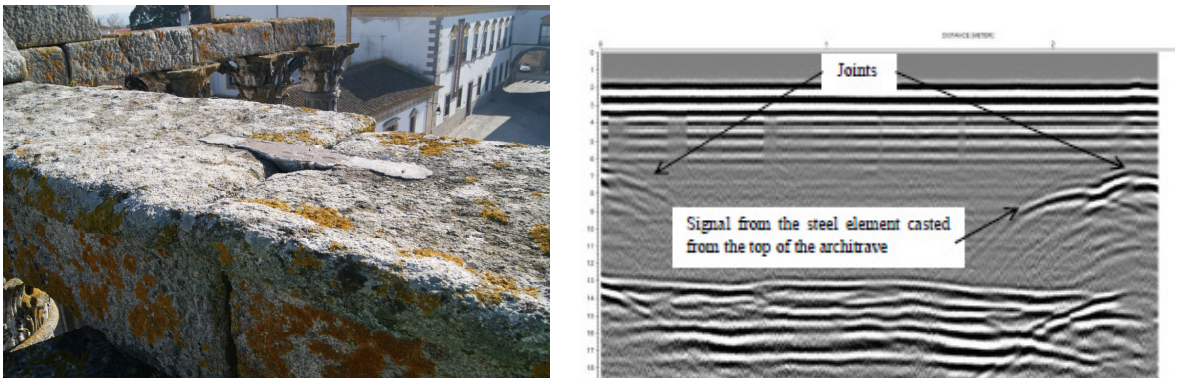

(a) (b)

Figure 3. Architraves: (a) metallic element identified during visual survey (b) GPR profile of top of respective architrave.

2.3. Dynamic identification

Dynamic identification tests were also conducted. The tests involved the placement of twelve uniaxial accelerometers throughout the structure in five different configurations, see Figure 4. Two tests were carried out for each configuration, the first test recorded only the ambient vibration, so as to be a baseline for analysis. The second test used a hammer to introduce an external excitation in the structure. Figure 5 provides the frequencies and damping ratios measured for one of the freestanding columns. This information was then used to calibrate the joint stiffness of the numeric models for discrete element analysis.

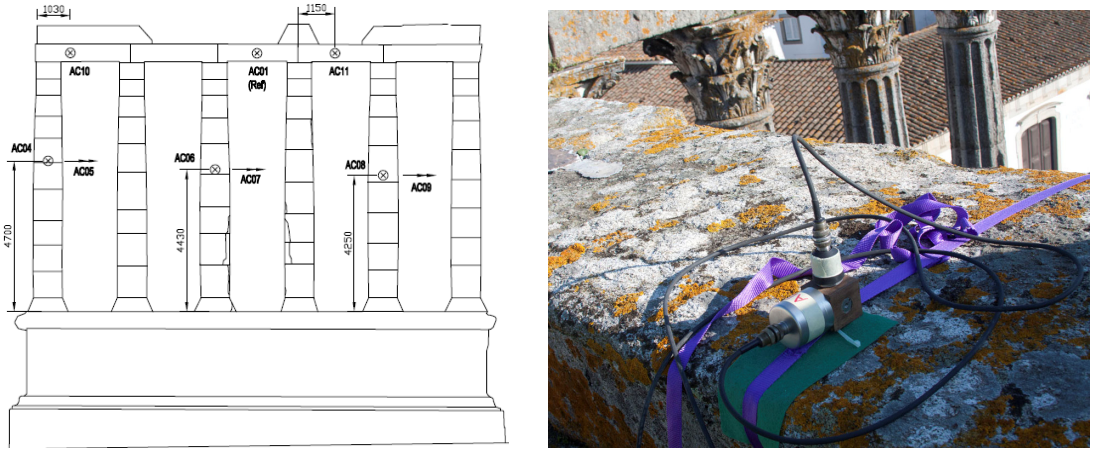

(a) (b)

Figure 4. Dynamic identification tests: (a) accelerometer positions for one test setup; (b) photograph showing accelerometers setup on top of architrave.

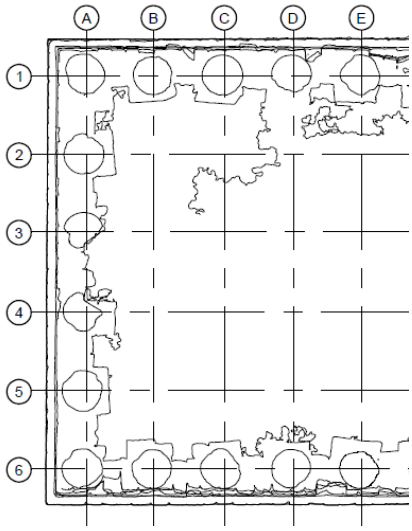

Natural frequency	Direction	Mode shape	Frequency	Average
1			2.80 Hz ξ = 2.1 %	3 Hz
			3.21 Hz ξ = 2.3 %	
2			16.25 Hz ξ = 2.0 %	17.5 Hz
			18.82 Hz ξ = 2.8 %	

(a) (b)

Figure 5. Experimental results: (a) Column grid references; (b) dynamic identification results of column E6.

3. MODELING

The structure was analysed using two different types of software, which have different degrees of complexity. This redundancy allows the results of models to be cross checked to obtain a better understanding of the structural behaviour of the temple. First, a limit analysis was conducted on the structure using the Block software (Orduña, 2004) and then static and dynamic analyses with 3DEC were undertaken (Itasca, 2000). Finally, a time history analysis using the discrete element method was carried out in order to evaluate the seismic behaviour of the structure. In both cases it was assumed that the blocks behave as rigid bodies where the joints have no tensile strength. It's also assumed that the blocks have limited compressive strength.

3.1. Limit analysis

The Block software allows the limit analysis of rigid block assemblages. Blocks can interact through frictional interfaces as it is observed in many historical masonry buildings. The model takes into account the cohesionless Coulomb criterion for the interfaces between blocks, where the shear stresses are tensionless and there is limited compressive strength. The purpose of the software is the seismic assessment of ancient masonry constructions made of blocks.

The temple was divided into 5 parts for analysis. All the analyses were based on two-dimensional models. First, the two freestanding columns D6 and E6 were analysed separately. Then, the three "façades" of the temple were analysed (East: E1 to A1; North: A1 to A6; West: A6 to C6). Since the structure is not symmetrical all of the models were studied with the earthquake applied in both directions. The model geometry did not take into account the ribs of the column drums. Equivalent cross-sectional areas were calculated in order to maintain equal volume throughout the blocks and thus the same mass. The tangent of the friction angle was taken as 0.7 and an effective compressive stress of 10 MPa was adopted.

The result obtained from the Block software was comprised of safety factors, thrust lines, and the failure mechanism. Table 1 summarizes the safety factors from the analysis. The following conclusions can be drawn from the results:

- The weakest sections of the temple appear to be within the main structure and not the freestanding columns. This is due to the fact that the architraves are not physically connected to the columns, therefore the architraves only add additional weight to the columns.
- The degree of acceleration that starts the collapse mechanism is approximately 0.1*g*. This approximation is very conservative as the temple is a slender structure, and the limit analysis does not take dynamic stability into account. This "dynamic stability" will be better observed with the discrete element dynamic analysis.

Table 1. Safety factors for an effective stress of 10 MPa.

	Earthquake direction (+)	Earthquake direction (-)
Column E6	0.12	0.12
Column D6	0.13	0.12
West side	0.11	0.10
North Side	0.10	0.11
East Side	0.10	0.10

Figure 6 shows the failure mechanisms obtained from the limit analysis using the block software with the horizontal load applied in the +x direction. The friction between the blocks ensures that the columns behave almost monolithically and dissipate energy during a seismic event.

3.2. Discrete element analysis

3.2.1. Calibration

In order for the 3DEC numerical models to produce accurate results, the material properties, primarily the joint normal and shear stiffnesses, must be calibrated. Here, the calibration was based on the natural frequencies obtained for the free standing column during the dynamic identification tests. Previous research by Lemos (2007) and Sincrain (2001) has shown that the shear stiffness can be assumed as half of the normal stiffness. Once this relationship was adopted, multiple numerical models were produced with different joint stiffnesses. The modal analysis produced frequency results that were then compared to the experimental results of the dynamic identification tests. Table 2 shows the material parameters used for the model. Since it was not possible to fully test the granite and marble materials to obtain the required properties, the mass density value in Table 2 was obtained from Vasconcelos (2005), whom tested granites from Portalegre, a region relatively close to Évora.

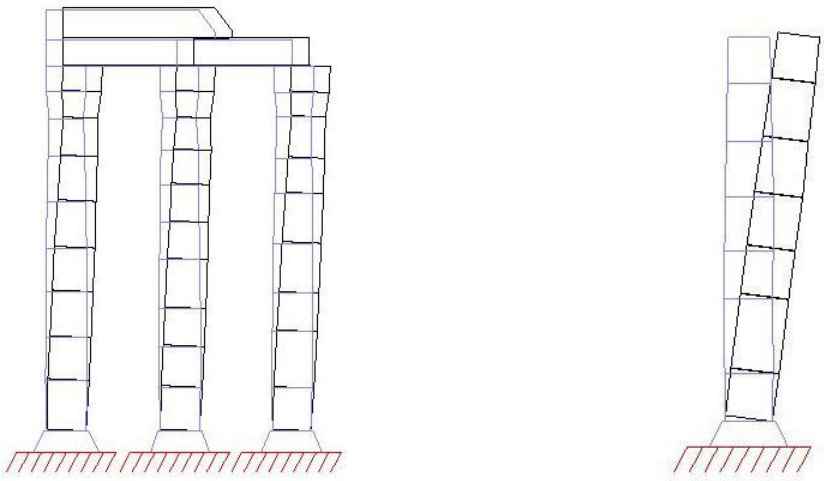

(a) (b)

Figure 6. Limit analysis failure mechanisms: (a) west façade; (b) freestanding column E6.

Table 2. Parameters of the free standing column.

Mass density (ton/m^3)	2.63
Normal joint stiffness (MPa/m)	3490
Shear joint stiffness (MPa/m)	1750
Friction angle (°)	35
Damping ratio (%)	2.2
First natural frequency (Hz)	2.8

3.2.2. Free standing column model

Once the calibration of the freestanding column was done, a series of time history analyses were run. The input accelerogram was designed according to Eurocode 8 EC8, for a PGA equal to 0.11*g* (NP EN 1998-1, 2010), considering the near field scenario as dominant. The generated accelerogram with duration of 14 seconds was converted into a velocity histogram and applied to the podium block in 3DEC. The discrete element analysis of the single freestanding column was conducted using a variation of earthquake PGA multipliers and joint stiffness properties. The analysis results show that the column fails due to rocking in the lower section of the column after the swaying, and fluctuates several times.

For a PGA multiplier factor of 2, the column did not explicitly fail, but the maximum displacement at the head of the column was 13.9 cm and the maximum residual displacement was approximately 4 cm. The results obtained by increasing the PGA multiplier show a similar qualitative response. The critical intensity of earthquake that causes failure of the column was estimated for a PGA multiplier factor around 7. Figure 7 shows the maximum displacement at the top as a function of the PGA multiplier. The values of normal joint stiffness and shear joint stiffness are equal to 3490 MPa/m and 1750 MPa/m, respectively.

As the earthquake intensity increases, the column response is dominated by rocking and sliding. Up to a PGA multiplying factor of 6, the magnified earthquake did not lead to collapse despite large displacements at the top of the structure. The maximum displacement reached 72 cm with a PGA multiplier factor of 6. It is noted that the maximum displacement at the top is significantly large enough to lead to failure in usual cases. However, the drums of the column did not fall because the column was subjected to the lateral force generated by the ground motion in the direction opposite to the displacement vector. Above a PGA multiplier factor of 7, however, the applied earthquakes led to column failure.

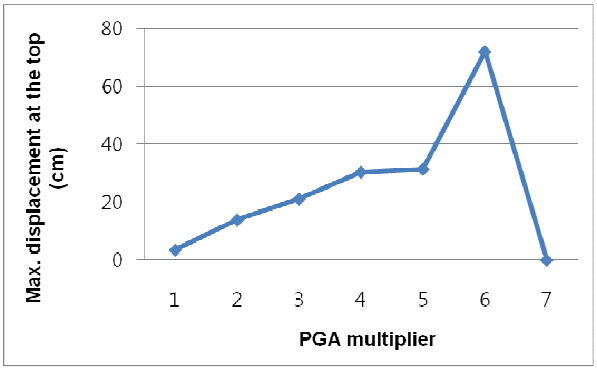

Figure 7. Maximum displacement of the top of freestanding column.

In order to estimate the influence of the joint stiffness on seismic response, the calibrated value of the joint stiffness (3490 MPa/m) was reduced and the smaller values were normalized and assigned to each analysis. Figure 8 shows the maximum displacement of the top with normalized joint stiffness's. A critical value of 25.5 MPa/m led to failure of the column excited by the non-magnified earthquake. The critical value of the normal stiffness was 0.73% of the calibrated normal joint stiffness.

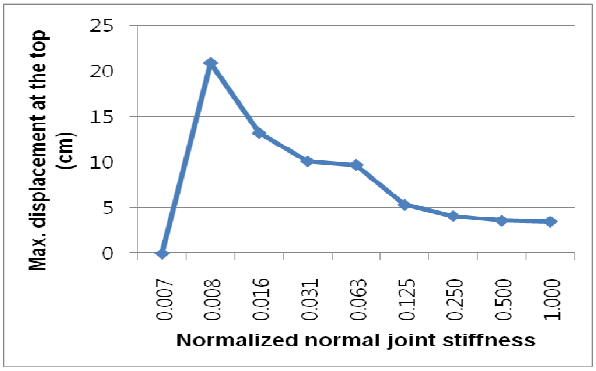

Figure 8. Maximum displacement of the top of freestanding column with varying joint stiffness.

3.2.3. Global model of the temple

A global model of the temple was set up and analysed in order to evaluate the seismic performance and failure mechanism of the entire structure under seismic excitation. The geometry of the global model was extracted from an existing 3D scan. Imperfections such as leaning and loss of cross-section area of columns were then modelled. Even though metallic connectors were identified at the top of some architraves during the site survey, the influence of the connectors was not taken into account since the geometry and material properties of the connectors were not investigated. Figure 9 illustrates the temple model with displacement monitoring positions labelled. The parameters of the model were those adopted for the single freestanding column, see also Table 2.

Table 3 presents the maximum seismic displacements, at each monitoring position, due to increasing PGA multiplier factors of the earthquake applied in the x-direction. The maximum displacement was monitored at positions 17 and 20. As expected, displacement increased with the increase of PGA multiplier factors.

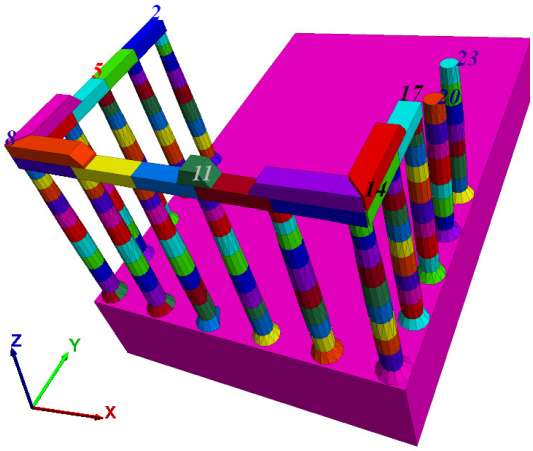

Figure 9. View of the temple model with monitoring points.

Table 3: Displacement response of monitoring positions (with indication of PGA multiplier factors).

PGA factor	collapse	Maximum displacement at the monitoring position (cm)							
		2	5	8	11	14	17	20	23
2	No	8.2	10	15.2	16.5	14.5	31	14.9	11
7	No	25	30	27.2	31.5	30.8	34	42.7	41.1
10	D6	47.3	47.3	46.4	51.7	48.9	65.9	failure	37.3

Figure 10 shows final states of the temple excited by earthquakes with PGA multiplier factors of 7 and 10, respectively. Up to a PGA multiplying factor of 7, the blocks of the model presented some residual displacements, after swaying without collapse. The results from a PGA multiplying factor of 10, however, showed that the ground motion induced failure for column D6. The results indicated that the columns connected by architraves show higher resistance than the freestanding columns. It is assumed that this was due to the fact that the additional loads provided by the architraves on the columns and the in-plane behaviour of the façade provides additional resistance against horizontal loads. The maximum displacement for a PGA multiplier factor of 7 was found at the monitoring position 20, located atop column D6, with a value of 42.7 cm in the x-direction, see Figure 10(a). The maximum displacement for a multiplier factor of 10, however, was measured at a point atop the architrave above column C6 (x-direction), with a value of 65.9 cm in the x-direction, as seen in Figure 10(b). This result does not include the failed column D6. In general, the severe loss of cross-sectional area of the lower part of columns A3 and A4 did not significantly affect the global behaviour.

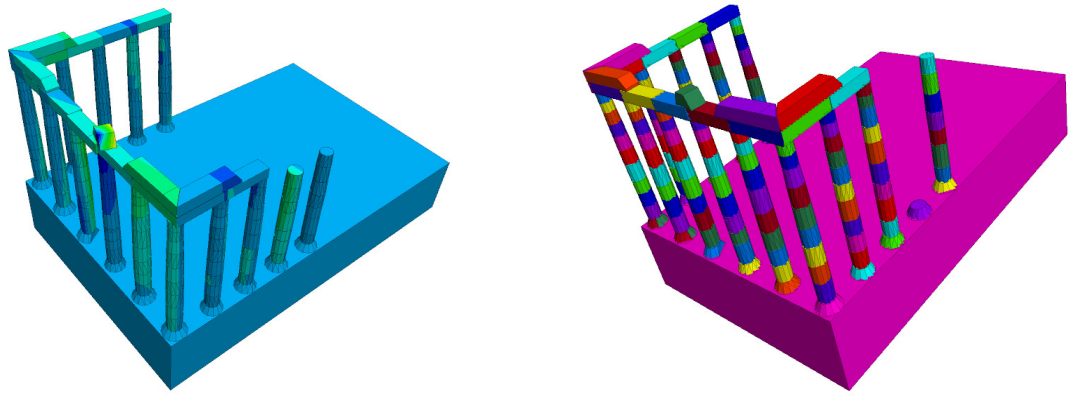

(a) (b)

Figure 10. Global response in x-direction: (a) PGA multiplier factor of 7; (b) PGA multiplier factor of 10.

3.2.4. Conclusion of failure mechanism analysis

From the results obtained for single freestanding column and the temple models, it can be qualitatively concluded that:

- The calibrated joint stiffness value is acceptable, however it might be a conservative overestimation.
- The acceptable values of normal joint stiffness range from about 870 to 3490 MPa/m.
- In the case of the near-field earthquake, the freestanding columns of the temple were able to resist strong earthquakes.
- Columns connected with architraves show higher resistance against horizontal forces than freestanding columns due to the additional weight of the architrave blocks.
- Out-of-plane behaviour of the temple façade and swaying of the free standing columns are critical to the global and local seismic responses.

4.CONCLUSION

The structural investigations described in this paper have led to the conclusion that the Roman temple is safer than was previously expected. A conservative limit analysis yielded failure mechanisms of the façades of the structure, however, the results from the DEM approach showed that the structure was extremely resistant to these mechanisms. Discrete element analysis also showed that the structure is very resistant to seismic action. The numerical model in 3DEC did not approach failure until the magnitude of the earthquake was multiplied by a factor of approximately 7. With magnification less than 7, excessive displacements did occur, however there were no collapses within the structure. This meant that the structure remained relatively stable and intact during seismic excitation many times larger in magnitude than that required of current Eurocode regulations for new structures.

Discrete element analysis also led to an interesting discovery regarding the rocking action of the blocks. While original assumptions let to believe that rocking would be detrimental to the stability of the structure, the opposite appeared true. The numerical models showed that even the freestanding columns constructed of independent blocks were more stable than expected. This is thought to be partially due to rocking of the blocks creating a mechanism to dissipate the energy from the seismic action.

The conclusions made from the discrete element dynamic analysis should be considered carefully, as there were some effects that were unable to be modelled. The models presented did not take the far field seismic action effects on the structure into account. In fact, due to time constraints related to the long processing times of the models, only near field excitation was modelled. Investigation to observe the results of far field excitation is currently being done. It must also be noted that the models do not include the iron clamps, as were observed connecting architraves. Exact material properties of these clamps were unknown and it was thought that the clamps would not have a significant effect on the global behaviour of the structure. Therefore, the clamps were not modelled.

With regards to biological colonization, only a general survey was conducted. Removal of the biological colonization was not discussed due to the conclusion that the current state of growth is of relatively low concern strictly regarding the structural system. More detailed investigations into treatment or removal of the biological colonization is advised for future interventions.

In terms of the intervention plans created as part of the broader project, the first proposal of the project would be to do nothing in terms of intervention. There is not enough evidence from the data obtained to suggest that the structure would be vulnerable to earthquakes expected in the region. This proposal, however, has to assume the risk that the structure may experience damage under severe seismic action. If that risk of collapse is still viewed as unacceptable, however, it was advised to implement a form of intervention.

AKCNOWLEDGEMENT

The work presented in this paper was developed within the framework of SAHC Erasmus Mundus Masters Course (www.msc-sahc.org) as a collaborative research between University of Minho and the Regional Directorate of Culture of Alentejo (DRCA). Authors are extremely grateful to those who have contributed to make this research possible, namely Dr. Vieira de Lemos (LNEC) for the assistance regarding discrete element method analysis; archaeologists Dr. Rafael Alfenim (DRCA) and Dr. Panagiotis Sarantopoulous (city council of Évora) for the valuable discussions and for sharing their knowledge; Dr. Ludovina Grilo (city council of Évora) for all the written material about the Roman temple and the city; Dr. Luís Mateus (Technical University of Lisbon) for the assistance in obtaining data from the 3D scans; Nuno Mendes and Dr. Francisco Fernandes (University of Minho) for assistance with dynamic identification and GPR tests, respectively; the SAHC program for creating this unique opportunity.

REFERENCES

NP EN 1998-1 (2010). Eurocódigo 8: Projecto de estruturas para resistência aos sismos – Parte 1: Regras gerais, acções sísmicas e regras para edifícios. Instituto Português da Qualidade.

Hauschild, T. (1997). El Templo Romano de Évora. Cuadernos de Arquitectura Romana , 107-117.

Hauschild, T. (1986). Intervenção efectuadas no templo de Évora no 1986. Trabalhos de Arqueologia do Sul , 93-98.

Hauschild, T. (1982). Zur Typologie Römischer Tempel auf der Iberischen Halbinsel. Peripterale Anlagen in Barcelona, Mérida und Évora. Homenaje a Saenz de Buruaga, Diputación Provincial de Badajoz , 145-156.

Itasca Consulting Group (2012). 3DEC: Numerical modeling code for advanced geotechnical analysis of soil, rock, and structural support in three dimensions.

Lemos, J. V. (2007). Discrete Element Modeling of Masonry Structures. International Journal of Architectural Heritage , 190-213.

Lopes, L., Lopes, J.C., Cabral, J.P., and Sarantopoulos, P. (2000). Caracterização Petrográfica dos Monumentos Romanos de Évora. A cidade de Évora II série, n.º 4 , 129-142.

Orduña, A. (2004). Seismic assessment of ancient Masonry structures by rigid block limit analysis. PhD thesis, University of Minho, Portugal.

Pereira, G. (1934). Estudos Diversos. Universidade de Coimbra.

Rodrigues, P. S. (2000). Giuseppe Cinatti e o restauro do Templo Romano de Evora. A cidade de Evora, II Serie, N° 4 , 273-287.

Sincraian, G.E. (2001). Seismic Behavior of Blocky Masonry Structures: A Discrete Element Method Approach. PhD Thesis, Technical University of Lisbon, Portugal.

Vasconcelos, G. (2005). Experimental investigations on the mechanics of stone masonry: characterization of granites and behavior of ancient masonry shear walls. PhD thesis.